Published in final edited form as:
Exp Eye Res. 2022 December ; 225: 109219. doi:10.1016/j.exer.2022.109219.

Ocular proteomic and transcriptomic changes with aging in a rabbit model of lensectomy with intraocular lens insertion

Jonathon B. Young[a,b], **Khalid Yusuf Al-Kirwi**[b], **Niamh Wynne**[b], **Amanda Rae Buchberger**[c,d], **Christine M.B. Skumatz**[b], **Ross F. Collery**[a,b], **Iris S. Kassem**[a,b,*]

[a]Cell Biology, Neurobiology, & Anatomy, Medical College of Wisconsin, Milwaukee, WI, USA

[b]Ophthalmology & Visual Sciences, Medical College of Wisconsin, USA

[c]Chemistry, University of Wisconsin-Madison, Madison, WI, USA

[d]Center for Biomedical Mass Spectrometry Research, Medical College of Wisconsin, Milwaukee, WI, USA

Abstract

Children that undergo intraocular surgery have an exaggerated postoperative response compared to adults that can result in significant postoperative challenges and reduced post-operative visual acuity. Rabbits were used as an animal model for investigating aging differences, treatment options, and surgical techniques for anterior chamber surgical interventions due to similarities in anterior chamber size and decreasing postoperative response with age. In our study, juvenile and adult rabbits underwent lensectomy with intraocular lens (IOL) insertion to determine how ocular RNA transcripts and proteins change with age. Rabbits underwent lensectomy with IOL insertion, and aqueous humor (AH) was collected immediately prior to surgery and at the peak of the postoperative response on post-operative day 3. Proteins related to coagulation and inflammation were assessed using targeted mass spectrometry. In addition, the cornea and iris/ciliary body tissues were dissected, and transcripts analyzed using RNA sequencing. While clinically, juvenile rabbits have greater fibrin formation following intraocular surgery compared to older rabbits, this change does not appear to be related to relative abundance levels of coagulation and inflammatory proteins in the AH. Gene transcript levels from a variety of immune response and inflammatory pathways reflected significant increases when comparing operated to unoperated ocular tissues, indicating the significant impact that surgery has on each ocular structure. This work further advances our understanding of how the rabbit eye proteomic and transcriptomic changes in response to surgery with aging, as we seek to ultimately identify the mechanisms for the exaggerated postoperative responses after pediatric intraocular surgery.

[*]Corresponding author. Medical College of Wisconsin, The Eye Institute, 925 N. 87th Street, Milwaukee, WI, 53226, USA. iriskassem@yahoo.com (I.S. Kassem).

Commercial relationship disclosures
None.

Appendix A. Supplementary data
Supplementary data to this article can be found online at https://doi.org/10.1016/j.exer.2022.109219.

Keywords

RNA Sequencing; Mass spectrometry; Coagulation; Inflammation; Rabbit; Cornea; Iris/ciliary body

1. Introduction

Cataract surgery is among the most common procedures performed in medicine, with over 20 million surgeries performed annually (Grzy-bowski, 2020). Due to numerous advances in the field of ophthalmology, adults often undergo routine cataract surgery without postoperative complications. Typically, cataract surgery is performed with insertion of an intraocular lens implant (IOL), resulting in positive visual outcomes in the immediate postoperative period for adults. Unlike adults, children with cataracts face unique obstacles, including an exaggerated post-operative response that can result in visually significant complications such as opacification of the visual axis due to membrane formation or scarring displacing the pupil to block central vision (Plager et al., 2011). In addition, younger children cannot have surgery delayed until there is a decreased risk of complications because deprivation amblyopia becomes more difficult to treat the longer a visually significant cataract remains untreated (Chan et al., 2012). Placement of an IOL in a young child at the time of cataract surgery may result in more complications, with the surgeon of young children choosing to perform lensectomy without IOL placement, known as aphakia (Plager et al., 2011). Despite the same IOL being placed in children and adults, the mechanisms underlying the differences of the pediatric and adult postoperative response to intraocular surgery with IOL implantation have not been elucidated.

Previous work has established the use of a juvenile rabbit model and demonstrated an increased abundance of inflammatory and coagulation cascade proteins in the aqueous humor (AH) following lensectomy with IOL implantation at the time of surgery (Young et al., 2020). Expanding on this work, we seek to establish how the abundance of inflammatory and coagulation proteins in the AH changes with increasing age using this rabbit animal model. Similar to humans, younger rabbits demonstrate a more robust postoperative response that decreases with age (Gwon, 2008). As older rabbits generate less of a postoperative response, we hypothesized that levels of coagulation and inflammatory proteins would be decreased in the AH compared to younger rabbits following intraocular surgery.

While proteomic differences associated with the exaggerated post-operative response have been described, the source of these proteins and how these proteins change in abundance with age, have yet to be identified. It is unknown if postoperative AH protein abundance changes arise from ocular structures, from the systemic circulation, or a combination of both. For example, fibrinogen chains and coagulation factors are known to be primarily produced in the liver and secreted into the circulation (Kopec and Luyendyk, 2014; Rizzo et al., 2019). However, despite being an avascular structure, there is evidence that the cornea is able to produce a variety of proteins related to the ocular immune response and coagulation, including complement components 3 and 9, along with Coagulation Factor

X and Prothrombin (Ayala et al., 2007; Dyrlund et al., 2012). Previous work performed by Ayala and colleagues revealed that both the proteins and mRNA for Prothrombin, Coagulation Factor X, and other coagulation co-factors are present in the cornea (Ayala et al., 2007). Ultimately, the latter report suggests that the cornea expresses components for vascular-independent production of thrombin, an essential protein within the fibrin formation pathway (Ayala et al., 2007; Loof et al., 2014).

Knowing that a variety of complement and coagulation components can be produced by the cornea itself, we sought to define how intraocular surgery may impact RNA transcripts of coagulation and inflammatory proteins in operated versus unoperated rabbit eyes with aging in a rabbit model of lensectomy. Although we recognize the limited correlation between transcriptomic and proteomic data (Haider and Pal, 2013; Liu et al., 2016) we sought to determine if coagulation and inflammatory transcripts in this structure are significantly altered and correlated with AH protein changes. As such a correlation may help identify a source of the protein abundance changes in the AH following surgery.

Carnes and colleagues previously performed transcriptome analysis of cornea and CB tissues in human fetal and adult ocular tissue (Carnes et al., 2018). Here, by examining how the levels of coagulation and inflammatory proteins and transcripts change following surgery in an aging rabbit model, we can further deduce the origins of the changing ocular response to lensectomy with increasing age. Conclusions from this study may further advance our understanding of the origins of the exaggerated postoperative response observed following pediatric intraocular surgery, yielding targets that may be localized to the ocular structures for long-term therapeutics.

2. Material and methods

2.1. Animal preparation & lensectomy

All experiments were approved and in compliance with the Institutional Animal Care and Use Committee (IACUC) at the Medical College of Wisconsin. A total of thirty-two New Zealand white rabbits, thirteen 5–7-weeks (juvenile rabbits) and nineteen 5–6-months of age (adult rabbits), from Kuiper Rabbit Farm (Gary, IN) were housed in a 14-h light, 10-h dark cycle and fed a diet of pelleted chow (Laboratory Rabbit Diet High Fiber 5326, LabDiet®, St. Louis, MO) daily and a Timothy hay cube twice per week (Bio-serv®, Flemington, NJ). Fourteen of the 32 rabbits (7 juvenile and 7 adult rabbits) did not undergo any surgical operation. Rabbits undergoing procedures for single-eye lensectomy with IOL implantation were anesthetized with isoflurane (5% induction, 2.5–4% maintenance) with 2 L per minute of oxygen for surgery and postoperative exams. Eyes were topically anesthetized with 0.5% tetracaine hydrochloride (Bausch & Lomb Inc., Tampa, FL) and dilated with 1% tropicamide and 2.5% phenylephrine (Akorn, Inc., Lake Forest, IL) before all procedures. The surgical technique, as described below, was standardized for every procedure, and the same surgeon performed all procedures for each experiment. The eye was prepped with 5% betadine solution (Alcon; Fort Worth, TX) placed into the eye. The surrounding area was prepped with 10% betadine and then draped. Preoperative (Pre) AH samples were collected via corneal paracentesis with a 27-gauge needle on a 1 mL tuberculin syringe. Pre

AH samples were then placed on ice and divided into 25 μL aliquots. Samples were then immediately stored at −80 °C until further analysis.

For lensectomy surgery for juvenile rabbits, after paracentesis, the anterior chamber was reformed with viscoelastic on a 27-gauge needle (Keralon™V++, Keragenix, Rapid City, SD). A clear corneal incision was made just anterior to the limbus using a 20-gauge MVR blade. A cystotome was used to puncture the anterior capsule followed by micro-utrata forceps to make a continuous curvilinear capsulorhexis. The soft juvenile lens was then removed by irrigation and aspiration with balanced salt solution (BSS® Sterile Irrigating Solution, Alcon Laboratories, Inc., Fort Worth, TX) via a Simcoe double lumen irrigation/aspiration cannula. There were no additional medications added to the solution. The anterior chamber and capsular bag were then filled with viscoelastic, and the wound was then expanded with a 2.4 mm keratome blade. A 10–0 nylon mattress suture was pre-placed into the corneal wound. A +30 diopter acrylic foldable intraocular lens (Alcon; Fort Worth, TX), was inserted into the capsular bag. The viscoelastic was then removed with Simcoe irrigation and aspiration. The preplaced suture was tied to close the wound, and the knot was buried. Sustained release subcutaneous buprenorphine (0.1 mg/kg) was given at the very end of the procedure for analgesia. The rabbit was then awakened from anesthesia and topical erythromycin was used twice daily for 4 days as antibiotic prophylaxis.

For the lensectomy surgery for adult rabbits, similar to the juvenile rabbits, after AH sampling with a paracentesis, the anterior chamber was reformed with viscoelastic on a 27-gauge needle, and a clear corneal incision was made just anterior to the lumbus using a 20-gauge MVR blade. The solid adult lens was broken apart by phacoemulsification using an Advanced Medical Optics (AMO) Sovereign White Star Phaco Machine (Advanced Medical Optics – now Johnson & Johnson Vision, Santa Ana, CA) using the “divide and conquer” technique where the lens was divided into sections and then removed (Gimbel, 1991). Following lens extraction, all remaining steps in the procedure are similar to those described above for the juvenile rabbits. Viscoelastic was used to fill the capsular bag, the 10–0 nylon mattress suture was pre-placed, and the +30 diopter acrylic foldable lens was inserted into the capsular bag. Viscoelastic was removed, the suture was buried, analgesia administered, and the rabbit was awakened from anesthesia.

2.2. Clinical examinations & ocular dissections

Postoperatively, rabbits were examined under sedation with isoflurane (as described above) on postoperative day 3 (POD 3), the peak day of the postoperative response determined in a previous manuscript (Bogaard et al., 2019). The same examiner performed all clinical exams. Slit lamp biomicroscopy (Topcon SL-D8Z; Topcon Medical Systems, Oakland, CA) was performed and photographs obtained using a Nikon D810 camera (Nikon, Melville, NY). Each eye was evaluated in the following categories: (1) iris synechiae, (2) pupil dilation in millimeters, and (3) presence or absence of hemorrhage in the anterior chamber. Anterior chamber inflammation was measured using cell and flare grade as per the SUN classification system criteria (Jabs et al., 2005). Following slit-lamp examination on POD 3, AH fluid was collected from the anterior chamber by corneal paracentesis as described above. Immediately after AH collection, rabbits were then euthanized with intravenous Fatal

Plus (Vortec Pharmaceuticals, Dearborn, MI) until death was confirmed with absence of respiration, cardiac function, corneal reflex, muscle tone, and mucus membrane color. The eyes were enucleated, then the cornea and iris/CB (note: the iris/CB were not separated) were dissected and placed in RNA*later* (Thermo Fisher Scientific, Waltham, MA) for RNA extraction at a later date. Ocular tissue from 14 rabbits that did not undergo any surgical operation were also harvested and dissected for control tissues.

2.3. Targeted quantitation of proteins of interest using tandem mass spectrometry

Paired AH samples from 6 juvenile rabbits and 5 adult rabbits were selected for mass spectrometry (MS) analysis. These numbers of samples were chosen based on a previous study where 5–6 rabbits per group revealed significant post-operative differences in coagulation proteins when analyzing AH fluid following different surgical interventions (Young et al., 2020). 10 µl of each AH sample was aliquoted and diluted with 100 mM ammonium bicarbonate, 40% Invitrosol, 20% acetonitrile (MeCN), and 5.52 mM tris(2-carboxyethyl)phosphine (TCEP) to bring the samples to a final concentration of 5 mM TCEP for reduction of the proteins. Samples were then incubated for 30 min at 1400 rpm at 25 °C in a thermomixer (Eppendorf, Hamburg, Germany). 100 mM iodoacetamide was added to bring samples to 10 mM for protein alkylation and then mixed in the dark for 30 min at 1400 rpm at 37 °C in a thermomixer. Pierce™ Trypsin/Lys-C (Thermo Scientific™, Waltham, MA) mix was added at a 1:20 trypsin-to-protein ratio for overnight incubation (~18 h) at 37 °C 1400 rpm in the thermomixer. Sera-Mag™ SpeedBead™ Carboxylate-Modified Magnetic Particles (hydrophylic and hydrophobic; GE Life Sciences, Sheffield, UK) were prepared at a 1:1 ratio to create a particle suspension, and peptides were prepared for proteomic analysis using the SP2 method as previously described (Waas et al., 2019). Briefly, 8 µl of particle solution was added to the samples to create a 20:1 particle to peptide ratio, and 100% MeCN was added to bring the final concentration of MeCN to 95%. Samples were mixed by pipetting up and down 3–5x to make sure the particles were well dispersed, allowed to settle for 2 min, and placed on a magnetic rack. The supernatant was removed, and samples were washed with 100% MeCN to cover the particles completely. Samples were returned to the magnetic rack and allowed to sit for 60 s. Next, another 100% MeCN wash was performed, and the supernatant discarded. The particles were then reconstituted in a solution consisting of 2% MeCN and water, vortexed, and allowed to settle for 1 min. The supernatant (now containing the peptides) was collected and transferred to a new microfuge tube. Samples were then acidified with 10% formic acid for a final concentration of 0.1% acid. The sample was then spun at 14000 rpm for 10 min to precipitate any remaining particles and the supernatant was collected.

Peptides were quantified using a Pierce™ Quantitative Fluorometric Peptide assay, and each sample was diluted to 25 ng/µl in 2% MeCN with 0.1% formic acid. Peptide Retention Time Calibration (PRTC) Mixture (Thermo Fisher Scientific, Waltham, MA) was added to each sample at a final concentration of 4 nM to enable retention time calibration and assessment of instrument performance throughout acquisition. Equal volumes of each sample were combined into a single “pooled quality-control (QC)” mixture.

Based upon a previous discovery study of AH proteins (Young et al., 2020), a selected list of 31 proteins of interest related to coagulation and complement cascades were analyzed by MS. The 31 proteins of interest were selected for a variety of reasons including quality of the separation, the number of peptides detected for specific proteins, the quality of the MS2 analysis and their relationship to coagulation and inflammatory cascades. A summary of MS methods is provided in Supplementary Fig. 1. Targeted quantitation by parallel reaction monitoring (PRM) was performed using a Dionex UltiMate 3000 RSLCnano system in-line with an Orbitrap Fusion™ Lumos™ Tribrid™ mass spectrometer. Samples (as two replicate injections) were queued in a randomized order. Each peptide was scheduled with a set 10-min scheduled retention time window, and resulting MS data were processed using Skyline (MacLean et al., 2010). All chromatography, instrumentation, and data processing settings can be found in Supplemental Table 1 and Supplemental Table 2. Retention times and ions were manually aligned and selected. Selected peptides and ions are reported in Supplemental Table 4 and on Skyline Panorama (https://panoramaweb.org/AZcKQZ.url). Identification of uncharacterized proteins or those with generic domains (such as cystatin domain-containing protein) were further validated by performing a protein Basic Local Alignment Search Tool (BLAST®) analysis of the FASTA sequence (Altschul et al., 1990).

2.4. RNA extraction, sequencing and transcriptome analysis

Ocular tissues from the six operated eyes of juvenile rabbits, seven juvenile unoperated control rabbit eyes, six operated adult rabbit eyes, and seven adult control rabbit eyes were processed for RNA sequencing. Corneas and iris/CB tissues were removed from RNA*later* and placed in pre-sterilized 2 mL free standing screw cap tubes (Fisher Scientific, Pittsburgh, PA) with 0.5 mm glass beads (Biospec Products, Inc., Bartlesville, OK) and 600 μl of Buffer RLT and 6 μl of β-mercaptoethanol reducing agent. Tissues were homogenized using a Mini-Bead beater 16 (Biospec Products) at 10 °C. Samples were homogenized for approximately 90 s and then cooled for 90 s on ice for three rounds. Following homogenization, RNA was extracted using a RNeasy® Extraction kit (Qiagen, Germantown, MD), according to the manufacturer’s protocol, with an additional wash step of 500 μl of Buffer RPE prior to adding the RNase-free water. Following this step, 50 μl of RNase-free water was added to the spin-column membrane to extract the total RNA. Samples were then frozen at −80 °C until further analysis.

Total RNA samples were sent to BGI Group (Shenzhen, China) for quality control verification and library preparation, and the subsequent steps document the work performed at the BGI laboratories. The Agilent 2100 Bio analyzer was used to determine the RNA concentration, RNA Integrity number (RIN), 28S/18S, and fragment length distribution. SOAPnuke software v1.5.2 (Chen et al., 2018) was used to filter reads, remove reads mapped to rRNAs, reads with adaptors, those in which unknown bases were more than 0.1%, and those defined as low quality (>40% of bases with quality of less than 20%). All samples included in this analysis were found to be of sufficient quantity (at least 1 μg) and had an RNA integrity number of at least 8.0 (Supplemental Table 3). Three operated cornea samples (one juvenile rabbit, two adult rabbits) were not included in the analyses due to insufficient quality. The DNBseq-G400 platform (Complete Genomics, 2015) was used for library preparation and sample sequencing. The reference genome was obtained from NCBI (version GCF_000003625.3). Clean reads were mapped to the reference genome using Bowtie2 (v2.2.5) (Langmead and Salzberg, 2012), and gene expression levels were calculated with RSEM (v1.2.12) (Li and Dewey, 2011).

Upon receiving the processed datasets, genes with a fragment per kilobase (FPKM) million >1 (in all samples within either the operated or unoperated groups) were included for further analysis. For select genes related to inflammatory and coagulation pathways, these FKPM values were directly compared between operated and unoperated eyes. Additional expression datasets generated based on rabbit age and type of ocular tissue, and FKPM values (Supplemental Table 5) were uploaded into Gene Set Enrichment Analysis software (v.4.0.3) (Subramanian et al., 2005). Gene sets were separated based on biological process, using the publicly available gene matrix (c5.bp.v6.1.symbols.gmt). The number of permutations was set to 1000, and there was no collapse to gene symbols. The “gene set” permutation type was used. Based on these parameters, gene sets with the highest normalized enrichment scores were further analyzed. This data has been deposited in the National Center for Biotechnology Information’s Gene Expression Omnibus (Edgar et al., 2002) and are accessible through GEO Series accession number GSE197306 (https://www.ncbi.nlm.nih.gov/geo/query/acc.cgi?acc=GSE197306).

2.5. Statistics

All statistical comparisons were performed using GraphPad Prism (v 9.0.0; GraphPad, La Jolla, CA). Categorical data assessments of cell and flare were compared using the Mann-Whitney *U* test with a p-value of <0.05 for significance. FKPM expression values for specific complementary and coagulation transcripts were compared using one-way analysis of variance (ANOVA) followed by post hoc Tukey test. All MS data were exported from Skyline and processed in MS stats (Choi et al., 2014) using the settings found in Supplementary Table 2. The average log intensity from the 2 replicate injections was calculated for each protein, and MS data were analyzed using with one-way analysis of variance (ANOVA) followed by post hoc Tukey test.

3. Results

3.1. Slit-lamp and clinical imaging

Following IOL insertion in the juvenile rabbits, a dense fibrin scar formed following surgery, completely occluding the visual axis (Fig. 1A), similar to the results observed in previous work (Young et al., 2020). In the adult rabbits, while the fibrin scar still formed, the area of the optic covered by fibrin appears reduced with slight scarring over the pupil in 8 of 12 rabbits. (Fig. 1B). Despite less fibrin formation, this did not result in significant differences in the clinically observed cell or flare grade between the age-groups (Fig. 1C and D).

3.2. Targeted mass spectrometry

Three days after lensectomy with IOL placement (POD 3), proteins related to the coagulation and the complement cascades demonstrated increased levels of abundance compared to preoperative samples. The specific abundances of selected complement and coagulation factors are provided in Fig. 3. Interestingly, the ratio of postoperative to preoperative protein abundance for a number of coagulation and inflammatory proteins was much greater for juvenile rabbits compared to adult rabbits (Fig. 2). Levels of Complement C1r, Prothrombin, Coagulation Factor V, and Coagulation Factor X were significantly increased between Pre and POD 3 samples for juvenile rabbits, but not adult rabbits (Fig. 3A, D, E, F). Coagulation Factor XI abundance was significantly increased between Pre and POD 3 for both age groups of rabbits (Fig. 3G). There was no significant difference in age-matched Pre and POD 3 abundance levels for Complement C3 and Complement C7 (Figs. 2 and 3). Levels of retinol-binding protein 3, a protein which may be involved with ocular immunosuppression (Young et al., 2020), significantly decreased following surgery for juvenile rabbits, but not adult rabbits (Fig. 3H).

Additional proteins assessed by targeted MS require further investigation to decipher their exact role in the post-operative response to lensectomy with IOL with aging (Supplementary Fig. 2). Many of these proteins remained relatively consistent in their abundance before and after surgery at both ages, thus rendering them potential control proteins to assess the quality of a MS sample.

3.3. Transcriptome analysis

There were 16,491 of 40,434 identified transcripts that met criteria of FPKM >1. Elevated levels of gene expression were observed for transcripts related to inflammatory and immune response pathways when comparing operated to unoperated ocular structures. Tables 1–4 reveal the top 5 biological pathways with the highest normalized enrichment scores based on age and the type of ocular tissue assessed. These pathways all had family wise error rate (FWER) p-values of 0. The complete table showing all ranked pathways for operated and unoperated tissue comparisons is provided in Supplemental Table 6. An example of genes upregulated within a listed pathway from Tables 1 and 3 and is provided in Fig. 4.

Specific transcripts related to immunomodulation, inflammation, and coagulation were also investigated (Fig. 5). In the iris/CB tissue, there was no significant difference in any complement component levels between juvenile and adult control eyes from unoperated rabbits. Complement C1r reflected differences between control eyes and operated eyes in juveniles and adults (Fig. 5A). Interestingly, Complement C4 (Fig. 5C) showed significant differences in gene expression between juvenile control eyes and juvenile operated eyes but no significant difference in adult eyes, while complement component 7 (Fig. 5D) presented differences in adult control eyes versus adult operated eyes, but no significant differences in juvenile eyes. Levels of transforming growth factor beta-2 (TGF-β2) significantly decreased following surgery in both age groups in the iris/CB.

In the cornea, complement C1r subcomponent (Fig. 5G) levels were significantly elevated in both age groups following surgery, but Complement C3 and C4 (Fig. 5 H, I) were only elevated in the juvenile operated group. No significant differences were observed in the age-matched operated versus control groups when assessing coagulation factors (Fig. 5E, J, K) for either tissue.

4. Discussion

The results presented in this work highlight a variety of key findings as we explore how the ocular immune system responds to surgery with age in this rabbit animal model. Although postoperative differences were not clinically observed between the cell and flare measurements (Fig. 1C and D) between ages, similar to young children having more complications related to intraocular scarring compared to adults, the area of the fibrin scar was reduced in adult rabbits compared to juvenile rabbits (Fig. 1A and B). We originally anticipated that a dense fibrin scar would correspond with a total higher abundance of complement and coagulation proteins in the juvenile rabbits compared to young adult rabbits. Interestingly, the preoperative levels of some coagulation factors appear to be higher in adult rabbits compared to juvenile rabbits. Following surgery, significant increases in these proteins were not observed, perhaps because the preoperative levels were already elevated and require further investigation.

Despite literature indicating systemic coagulation factors are lower in children and increase with age (Abbate et al., 1993; Appel et al., 2012), fibrin scar formation remains a problem in children, but not adults, undergoing intraocular cataract procedures. Additional aging studies should be performed to accurately determine how these coagulation proteins change in unoperated/control rabbits with age both in the AH and systemically. If the levels of these proteins continue to increase in older adult rabbits, this may suggest that the proportion of the increase in abundance compared to baseline levels of these inflammatory and coagulation proteins may drive formation of the fibrin scar, rather than the absolute abundance of the proteins themselves. Exploring the mechanisms of aging in operated and non-operated eyes in a rabbit model can help deduce the underlying causes of this fibrin formation in children. This will inform future translational research targeting the coagulation or inflammatory cascades to improve post-operative outcomes in patients that are high-risk such as intraocular surgery in children or uveitis patients.

In previous work from our laboratory, we reported a significant decrease in the levels of the protein TGF-β2 in the AH following lensectomy with primary IOL insertion (Young et al., 2020). Here, we report that transcripts of TGF-β2 were also significantly decreased in the iris/CB ocular structures at both age groups following surgery (Fig. 5F). While TGF-β2 has been previously reported to be present in the AH (Jampel et al., 1990), the source of the TGF-β2 has yet to be explicitly identified. If the source of TGF-β2 is the iris or CB and is constitutively produced, the lack of TGF-β2 production after lensectomy could therefore result in less TGF-β2 in the AH, leading to less immunosuppression in the anterior chamber, ultimately releasing inhibition and leading to an exaggerated immune response.

Complement and coagulation proteins have been previously identified in the cornea (Ayala et al., 2007; Dyrlund et al., 2012) and the AH (Young et al., 2020). In this work, we sought to determine how intraocular surgery would impact their transcripts in the iris/CB and cornea both being tissues that could be the source of these proteins in the AH. Genes from a variety of immune-response and inflammatory pathways reflected significant increases in transcription levels when comparing operated to unoperated ocular tissues (Tables 1–4), indicating the significant impact that surgery had on each ocular structure. We then analyzed specific inflammatory and coagulation transcripts that shared genes with the proteins identified within the MS dataset. Surprisingly, in the coagulation factors identified that met analysis criteria, there were no significant differences in pre- and post-operative levels between control eyes and operated eyes in either set of ocular tissues (Fig. 5 E, J and K). While complement transcripts in the cornea may be increasing, this does not appear to be consistent with the increased abundance of that protein in the AH. Evaluating the coagulation and complement protein levels themselves within the ocular structures with MS would help determine if the surgery alters transcript levels only, or if the procedure also alters protein expression for the structure as well, allowing for the source of the AH protein to be further defined.

A previous study of this model involved clinical examination from POD 3–14 inclusive (Bogaard et al., 2019). The findings of this study included the observation of peak post-operative response on POD 3. This finding informed choice of POD 3 for examination in subsequent quantitative proteomic studies (Young et al., 2020, 2021). In order to facilitate comparison with the existing body of work in this model we continued with the selection of POD 3 for these experiments.

Although informative regarding the changes of inflammatory and coagulation proteins in the AH, along with studying the transcripts in operated and unoperated ocular structures with increasing age, this study did have limitations. First, studying an even older rabbit age (such as 12 months), may provide key data to document how normative levels of coagulation and complement proteins may change in abundance in the AH with advanced age. Determining how these proteins change in abundance following lensectomy in a 12-month rabbit could help further deduce if concentrations of these proteins or their relative change in abundance are responsible for the exaggerated postoperative response. Second, conclusions from mRNA and protein studies must be carefully considered due to multiple avenues of transcriptional and translational regulation of protein abundance, as well as post-translational modifications (Liu et al., 2016). Determining the presence and abundance of coagulation and inflammatory proteins in the ocular tissues themselves in surgically naive and operated rabbits may indicate whether these tissues are the direct source of protein collected in the AH sample. Third, this analysis only included transcripts with FPKM values > 1 in all samples within an operated or control group. We recognize other transcripts of interest may not have been included in this first analysis and will require further investigation as mechanisms and insights related to the RNA-sequencing dataset continue to be explored. Lastly, although an ideal model for studying anterior segment ophthalmic investigations, New Zealand White rabbits are unpigmented and exhibit less genetic variability compared to humans, and these factors need to be born in mind when interpreting these studies.

While there is evidence of limited correlation between transcriptome and proteome, we did not perform an analysis of this correlation as part of this work. Our study used targeted MS to examine specific, preselected peptides derived from proteins of interest. Thus, these peptides are assumed to be representative of the abundance of the proteins of interest for the purposes of this work. Given this assumption, further direct correlation between these targeted peptides and the whole transcriptome may infer imperfect results. Future work to elucidate full proteome data would allow such correlation to be interrogated.

This work establishes that both proteomic and transcriptomic changes occur in the AH fluid and ocular structures following lensectomy with IOL insertion, and that some changes such as the postoperative to preoperative abundance ratio of select coagulation and complement proteins, change with aging. This work further advances our understanding of how the eye changes its response to surgery with age as we seek to ultimately identify the mechanisms responsible for the exaggerated postoperative responses in pediatric intraocular surgery procedures. The results of these studies further support the potential of targeting the coagulation and complement pathways as well as other unique therapeutic targets to improve postoperative outcomes after lensectomy in children, potentially improving visual outcomes for children and other high-risk patients.

Supplementary Material

Refer to Web version on PubMed Central for supplementary material.

Acknowledgements

The authors thank Michael Pereckas (Center for Biomedical Mass Spectrometry Research, Medical College of Wisconsin) for their assistance regarding sample preparation and analysis for the mass spectrometry components of this work.

Disclosure of funding

Research in this publication was supported in part by the National Eye Institute of the National Institutes of Health under awards K08EY024645 (ISK), P30EY001931, and C06RR016511.

Data availability

Data will be made available on request.

References

Abbate R, Prisco D, Rostagno C, Boddi M, Gensini GF, 1993. Age-related changes in the hemostatic system. Int. J. Clin. Lab. Res 23, 1–3. [PubMed: 8477086]

Altschul SF, Gish W, Miller W, Myers EW, Lipman DJ, 1990. Basic local alignment search tool. J. Mol. Biol 215, 403–410. [PubMed: 2231712]

Appel IM, Grimminck B, Geerts J, Stigter R, Cnossen MH, Beishuizen A, 2012. Age dependency of coagulation parameters during childhood and puberty. J. Thromb. Haemostasis 10, 2254–2263. [PubMed: 22909016]

Ayala A, Warejcka DJ, Olague-Marchan M, Twining SS, 2007. Corneal activation of prothrombin to form thrombin, independent of vascular injury. Investig. Ophthalmol. Vis. Sci 48, 134–143. [PubMed: 17197526]

Bogaard JD, Young JB, Movahedan A, Kassem IS, 2019. Use of a juvenile rabbit animal model to evaluate therapeutic interventions for postoperative inflammation and fibrin formation after lensectomy. Transl. Vision Sci. Technol 8, 5.

Carnes MU, Allingham RR, Ashley-Koch A, Hauser MA, 2018. Transcriptome analysis of adult and fetal trabecular meshwork, cornea, and ciliary body tissues by RNA sequencing. Exp. Eye Res 167, 91–99. [PubMed: 27914989]

Chan WH, Biswas S, Ashworth JL, Lloyd IC, 2012. Congenital and infantile cataract: aetiology and management. Eur. J. Pediatr 171, 625–630. [PubMed: 22383071]

Chen Y, Chen Y, Chunmei S, Huang Z, Zhang Y, Li S, Li Y, Ye J, Yu C, Li Z, Zhang X, Wang J, Yang H, Fang L, Chen Q, 2018. SOAPnuke: a MapReduce acceleration-supported software for integrated quality control and preprocessing of high-throughput sequecing data. GigaScience 7, 120.

Choi M, Chang CY, Clough T, Broudy D, Killeen T, MacLean B, Vitek O, 2014. MSstats: an R package for statistical analysis of quantitative mass spectrometry-based proteomic experiments. Bioinformatics 30, 2524–2526. [PubMed: 24794931]

Complete Genomics, I., 2015. Revolocity Whole Genome Sequencing Technology Overview [Brochure]. USA.

Dyrlund TF, Poulsen ET, Scavenius C, Nikolajsen CL, Thogersen IB, Vorum H, Enghild JJ, 2012. Human cornea proteome: identification and quantitation of the proteins of the three main layers including epithelium, stroma, and endothelium. J. Proteome Res 11, 4231–4239. [PubMed: 22698189]

Edgar R, Domrachev M, Lash AE, 2002. Gene expression omnibus: NCBI gene expression and hybridization array data repository. Nucleic Acids Res. 30, 207–210. [PubMed: 11752295]

Gimbel HV, 1991. Divide and conquer nucleofractis phacoemulsification: development and variations. J. Cataract Refract. Surg 17, 281–291. [PubMed: 1861242]

Grzybowski A, 2020. Recent developments in cataract surgery. Ann. Transl. Med 8, 1540. [PubMed: 33313285]

Gwon A, 2008. The rabbit in cataract/IOL surgery. In: Tsonis P. (Ed.), Animal Models in Eye Research. Elsevier, pp. 184–204.

Haider S, Pal R, 2013. Integrated analysis of transcriptomic and proteomic data. Curr. Genom 14, 91–110.

Jabs DA, Nussenblatt RB, Rosenbaum JT, Standardization of Uveitis Nomenclature Working, G, 2005. Standardization of uveitis nomenclature for reporting clinical data. Results of the First International Workshop. Am. J. Ophthalmol 140, 509–516. [PubMed: 16196117]

Jampel HD, Roche N, Stark WJ, Roberts AB, 1990. Transforming growth factor- beta in human aqueous humor. Curr. Eye Res 9, 963–969. [PubMed: 2276273]

Kopec AK, Luyendyk JP, 2014. Coagulation in liver toxicity and disease: role of hepatocyte tissue factor. Thromb. Res 133 (Suppl. 1), S57–S59. [PubMed: 24759146]

Langmead B, Salzberg SL, 2012. Fast gapped-read alignment with Bowtie 2. Nat. Methods 9, 357–359. [PubMed: 22388286]

Li B, Dewey CN, 2011. RSEM: accurate transcript quantification from RNA-Seq data with or without a reference genome. BMC Bioinf. 12, 323.

Liu Y, Beyer A, Aebersold R, 2016. On the dependency of cellular protein levels on mRNA abundance. Cell 165, 535–550. [PubMed: 27104977]

Loof TG, Deicke C, Medina E, 2014. The role of coagulation/fibrinolysis during Streptococcus pyogenes infection. Front. Cell. Infect. Microbiol 4, 128. [PubMed: 25309880]

MacLean B, Tomazela DM, Shulman N, Chambers M, Finney GL, Frewen B, Kern R, Tabb DL, Liebler DC, MacCoss MJ, 2010. Skyline: an open source document editor for creating and analyzing targeted proteomics experiments. Bioinformatics 26, 966–968. [PubMed: 20147306]

Plager DA, Lynn MJ, Buckley EG, Wilson ME, Lambert SR, Infant Aphakia Treatment Study, G., 2011. Complications, adverse events, and additional intraocular surgery 1 year after cataract surgery in the infant Aphakia Treatment Study. Ophthalmology 118, 2330–2334. [PubMed: 21925737]

Rizzo K, Vella K, Zammit D, Gatt P, Grima C, Inguanez MB, Gerada J, Ellul P, Vassallo M, Azzopardi N, Pocock J, Gatt A, 2019. Fibrinogen measurement in liver disease: validation of the functional fibrinogen thromboelastography assay and a novel mathematical predictive model. Blood Transfusion 17, 237–246. [PubMed: 30418134]

Subramanian A, Tamayo P, Mootha VK, Mukherjee S, Ebert BL, Gillette MA, Paulovich A, Pomeroy SL, Golub TR, Lander ES, Mesirov JP, 2005. Gene set enrichment analysis: a knowledge-based approach for interpreting genome-wide expression profiles. Proc. Natl. Acad. Sci. U.S.A 102, 15545–15550. [PubMed: 16199517]

Waas M, Pereckas M, Jones Lipinski RA, Ashwood C, Gundry RL, 2019. SP2: Rapid and automatable contaminant removal from peptide samples for proteomic analyses. J. Proteome Res 18, 1644–1656. [PubMed: 30795648]

Young JB, Buchberger AR, Bogaard JD, Berg Luecke L, Runquist M, Skumatz CMB, Kassem IS, 2021. Tissue plasminogen activator effects on fibrin volume and the ocular proteome in a juvenile rabbit model of lensectomy. Transl. Vision Sci. Technol 10, 7.

Young JB, Keppel TR, Waas M, Salmon AE, Buchberger AR, Skumatz CMB, Gundry RL, Kassem IS, 2020. Quantitative proteomic analysis of aqueous humor after rabbit lensectomy reveals differences in coagulation and immunomodulatory proteins. Mol Omics 16, 126–137. [PubMed: 32031200]

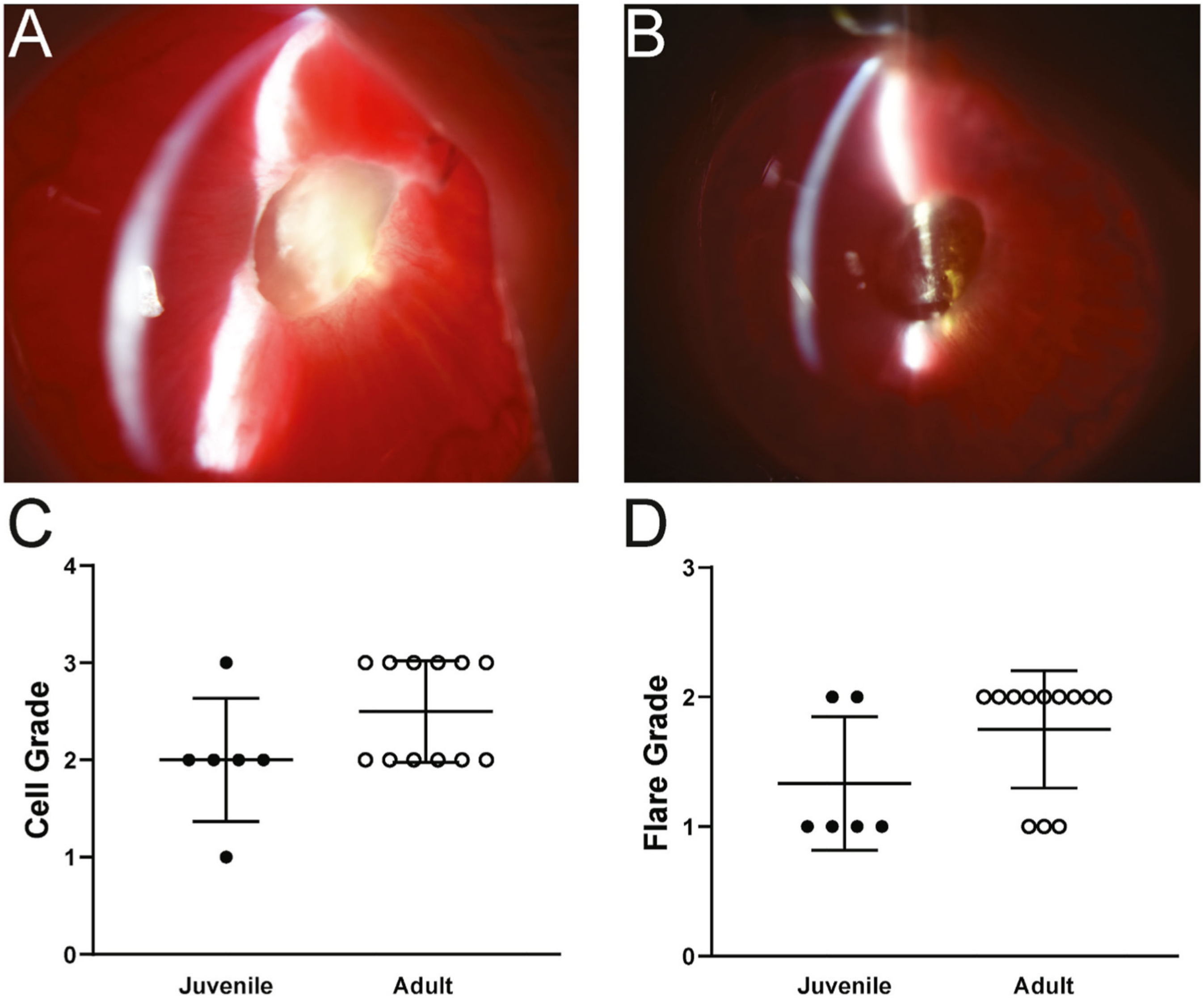

Fig. 1. Clinical examinations following lensectomy with IOL insertion in an aging rabbit model.
Representative color pictures of rabbit eyes following lensectomy with IOL insertion on POD 3 for juvenile (6 week-old rabbits; **A**) and adult (6 month-old; **B**). Despite less fibrin scar formation observed in adult rabbits, this did not result in significant changes to cell or flare measurements (**C** and **D**).

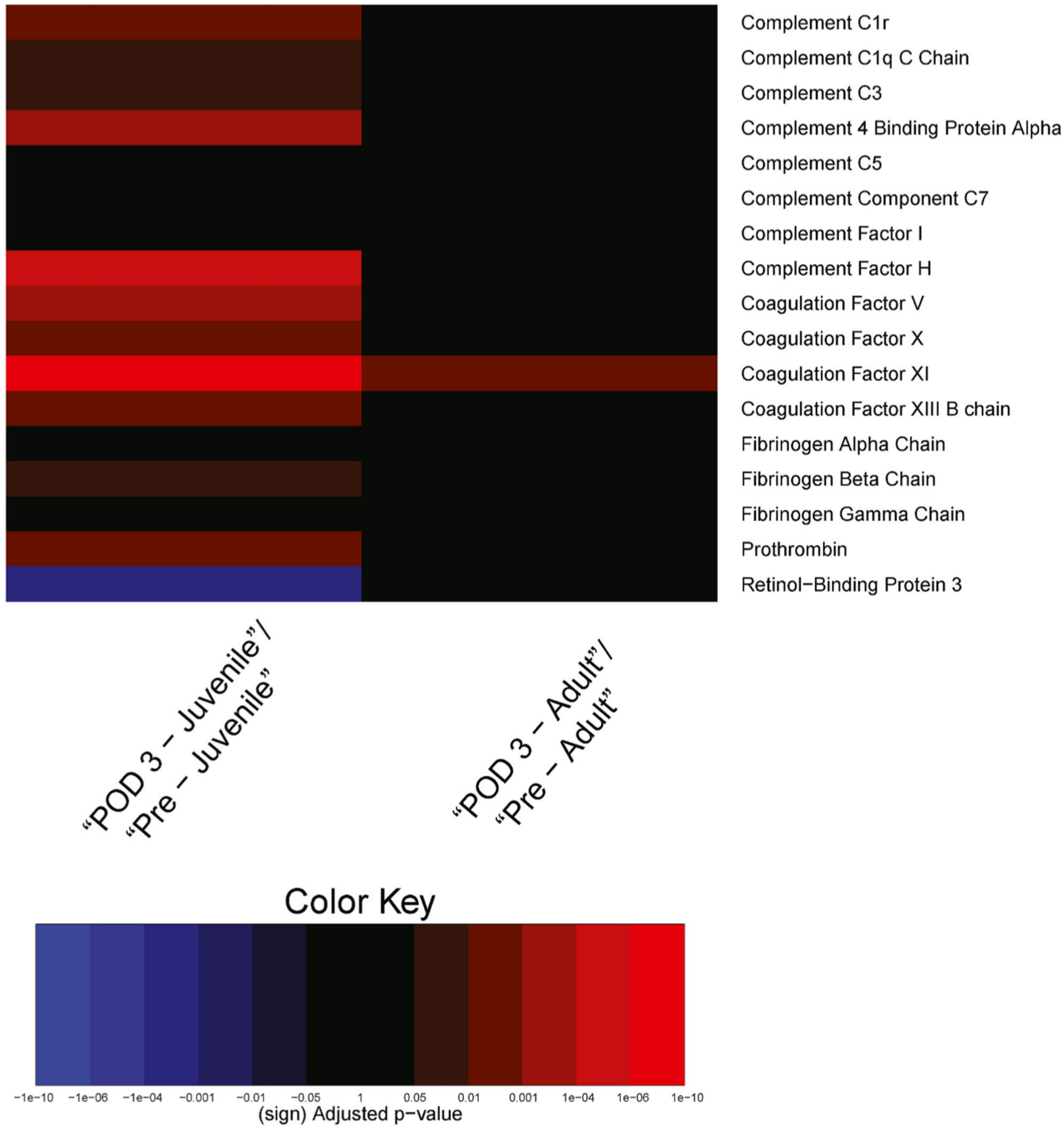

Fig. 2. Heatmap of proteins relative to preoperative levels.

Proteins related to the coagulation pathway and complement cascade generally increased in abundance or remained similar to preoperative levels for both age groups. Juvenile rabbits demonstrated greater changes in postoperative to preoperative protein abundances compared to adult rabbits.

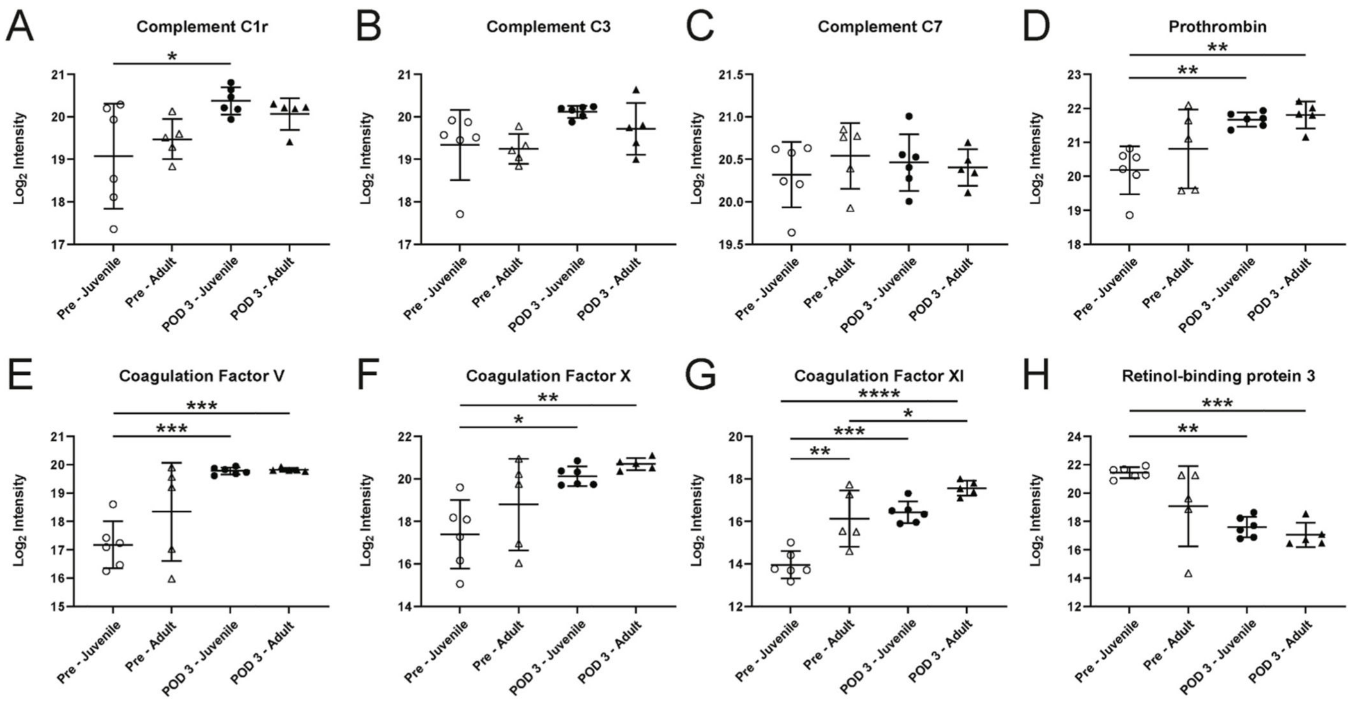

Fig. 3. Protein abundances assessed by MS.

A variety of proteins related to coagulation and inflammation (complement proteins) were significantly different between Pre and POD 3 for the 6 week-old rabbits. Coagulation Factor XI was the only protein with differences in the 6 month-old Pre and 6 month-old POD 3 samples. One juvenile rabbit had only one technical replicate available for analysis for Coagulation Factor XI, but all other rabbits had two technical replicates as noted above. (The sample with one technical replicate was not uploaded to Panorama). Graphs represent the average ± SD; *p < 0.05, **p < 0.01, ***p < 0.001, ****p < 0.0001.

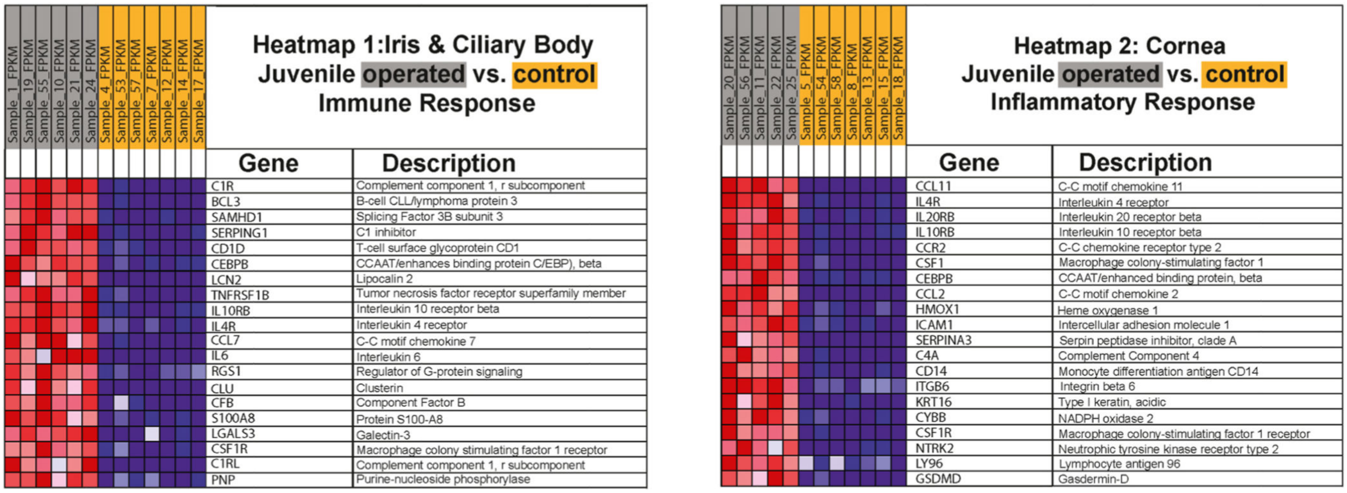

Fig. 4. Representative heatmaps from pathways

in Tables 1 and 3 Transcripts related to the inflammatory response and immune response were significantly upregulated in operated eyes (columns in gray) compared to unoperated eyes (columns in yellow). Darker shades of red indicate higher levels of gene expression, while darker shades of blue indicate lower levels of gene expression.

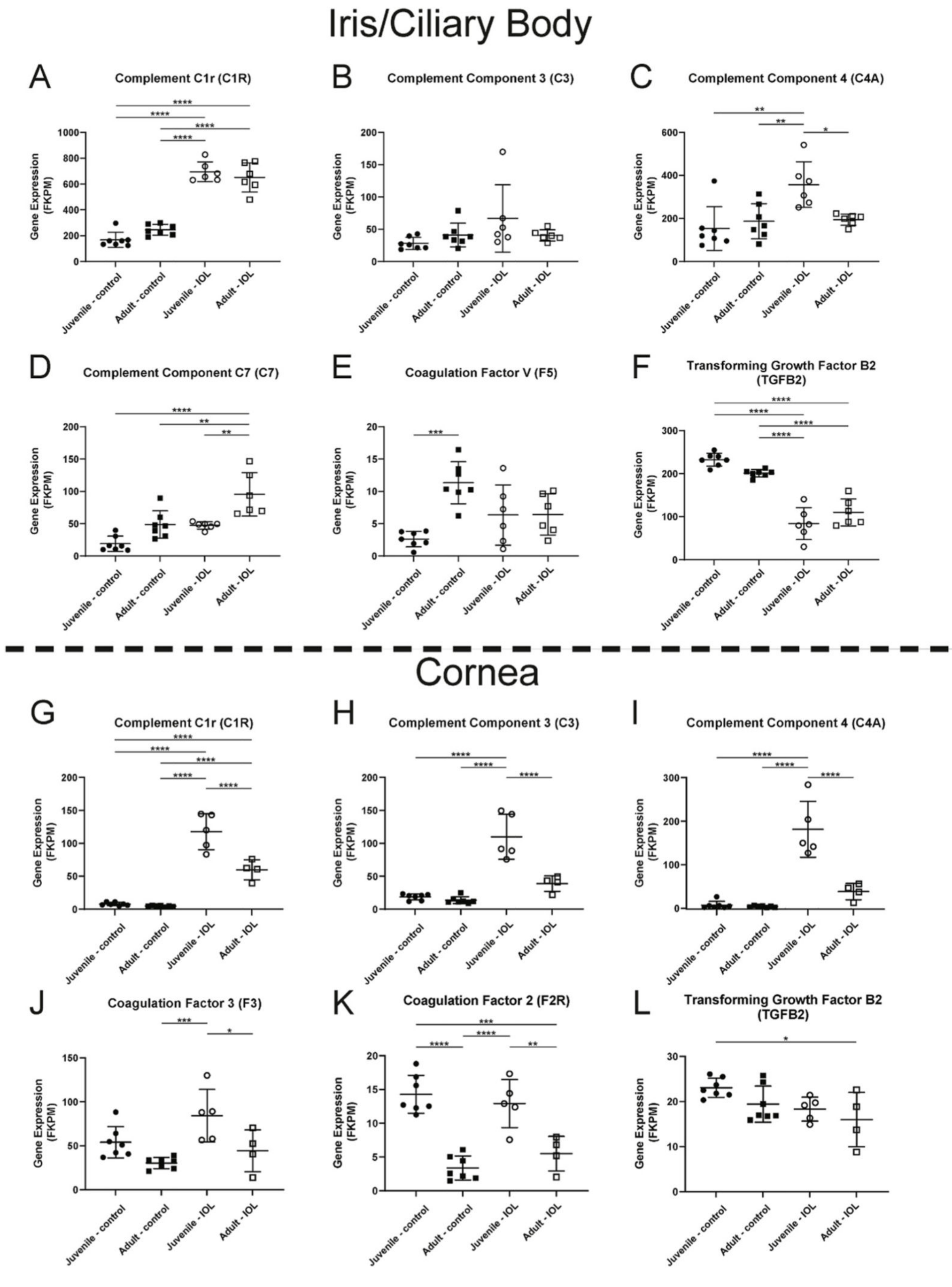

Fig. 5. Gene expression values for inflammation, coagulation and immunomodulatory proteins of interest.

Transcripts expressed from the iris & CB tissues are reported in panels A–F, and transcripts from the cornea and shown in panels G–L. The specific gene name is provided in parenthesis. FPKM values are reported as average ± SD; *p < 0.05, **p < 0.01, ***p < 0.001, ****p < 0.0001.

Author Manuscript
Author Manuscript
Author Manuscript

Table 1

Normalized Enrichment Scores for Iris & Ciliary Body

6 week-old rabbits – operated vs. non-operated tissues.

Rank	Gene Set (Gene Ontology)	Size	Enrichment Score	Normalized Enrichment Score	Nominal p-value	FDR q-value
1	Immune Response	498	0.586	2.742	0	0
2	Innate Immune Response	273	0.62	2.741	0	0
3	Inflammatory Response	242	0.625	2.73	0	0
4	Positive Regulation of Cytokine Production	210	0.611	2.627	0	0
5	Regulation of Cytokine Production	335	0.56	2.526	0	0

Table 2

Normalized Enrichment Scores for Iris & Ciliary Body
6 month-old rabbits – operated vs. non-operated tissues.

Rank	Gene Set (Gene Ontology)	Size	Enrichment Score	Normalized Enrichment Score	Nominal p-value	FDR q-value
1	Inflammatory Response	242	0.595	2.785	0	0
2	Immune Response	498	0.54	2.749	0	0
3	Cell Cycle G1-S-phase transition	86	0.658	2.701	0	0
4	Positive Regulation of Cytokine Production	210	0.576	2.69	0	0
5	Regulation of Cytokine Production	273	0.557	2.663	0	0

Author Manuscript

Author Manuscript

Author Manuscript

Table 3

Normalized Enrichment Scores for Cornea

6 week-old rabbits – operated vs. non-operated tissues.

Rank	Gene Set (Gene Ontology)	Size	Enrichment Score	Normalized Enrichment Score	Nominal p-value	FDR q-value
1	Inflammatory Response	202	0.665	2.734	0	0
2	Leukocyte Chemotaxis	47	0.789	2.593	0	0
3	Cell Chemotaxis	72	0.734	2.581	0	0
4	Regulation of Leukocyte Migration	69	0.715	2.514	0	0
5	Myeloid Leukocyte Migration	40	0.778	2.495	0	0

Table 4

Normalized Enrichment Scores for Cornea

6 month-old rabbits – operated vs. non-operated tissues.

Rank	Gene Set (Gene Ontology)	Size	Enrichment Score	Normalized Enrichment Score	Nominal p-value	FDR q-value
1	Immune Response	427	0.52	2.754	0	0
2	Innate Immune Response	251	0.537	2.709	0	0
3	Inflammatory Response	202	0.556	2.703	0	0
4	Response to Cytokines	381	0.513	2.693	0	0
5	Positive Regulation of Leukocyte Chemotaxis	37	0.75	2.676	0	0